CHEMMEDCHEM
COMMUNICATIONS

ChemPubSoc
Europe

DOI: 10.1002/cmdc.201400045

The Discovery of Potent Nonstructural Protein 5A (NS5A) Inhibitors with a Unique Resistance Profile—Part 1

Thien Duc Tran,[a] Florian Wakenhut,[a] Chris Pickford,[b] Stephen Shaw,[b] Mike Westby,[b] Caroline Smith-Burchnell,[b] Lesa Watson,[a] Michael Paradowski,[a] Jared Milbank,[a] Rebecca A. Brimage,[d] Rebecca Halstead,[d] Rebecca Glen,[d] Craig P. Wilson,[d] Fiona Adam,[a] Duncan Hay,[a] Jean-Yves Chiva,[a] Carly Nichols,[a] David C. Blakemore,[a] Iain Gardner,[c] Satish Dayal,[c] Andrew Pike,[c] Rob Webster,[c] and David C. Pryde*[a]

Nonstructural protein 5A (NS5A) represents a novel target for the treatment of hepatitis C virus (HCV). Daclatasvir, recently reported by Bristol–Myers–Squibb, is a potent NS5A inhibitor currently under investigation in phase 3 clinical trials. While the performance of daclatasvir has been impressive, the emergence of resistance could prove problematic and as such, improved analogues are being sought. By varying the biphenyl-imidazole unit of daclatasvir, novel inhibitors of HCV NS5A were identified with an improved resistance profile against mutant strains of the virus while retaining the picomolar potency of daclatasvir. One compound in particular, methyl ((*S*)-1-((*S*)-2-(4-(4-(6-(2-((*S*)-1-((methoxycarbonyl)-L-valyl)pyrrolidin-2-yl)-1*H*-imidazol-5-yl)quinoxalin-2-yl)phenyl)-1*H*-imidazol-2-yl)-pyrrolidin-1-yl)-3-methyl-1-oxobutan-2-yl)carbamate (**17**), exhibited very promising activity and showed good absorption and a long predicted human pharmacokinetic half-life. This compound represents a promising lead that warrants further evaluation.

It is estimated that some 3% of the world's population is currently infected with hepatitis C virus (HCV).[1] Approximately 70% of infected individuals develop a chronic infection, a portion of whom go on to develop chronic liver disease.[2] While the rate of new infections has declined sharply in the last two decades, the need for broadly efficacious and well-tolerated therapies remains high. Standard of care therapy for many years was a combination of injected pegylated interferon and ribavirin, which can eradicate the virus with varying degrees of success depending on the genotype of virus the patient is infected with, and other genetic factors.[3] Genotype 1 (gt1), the most prevalent genotype in Europe and the US, responds only modestly to interferon therapy with a sustained virologic response in approximately half of the treated population, and the treatment is associated with severe side effects and significant discontinuation rates. Recent approvals of drugs that target alternative antiviral mechanisms include the protease inhibitors telaprevir, boceprevir and simeprevir, and the polymerase inhibitor sofosbuvir, bringing the prospect of interferon-sparing treatment regimens closer.[4]

To make this a reality, new effective antivirals are required that will allow a phasing out of interferon-based regimens to be replaced with better tolerated medicines. HCV is also a highly mutable virus, and as resistance mutations emerge, new and effective antiviral mechanisms will be needed.

The single-stranded RNA genome of HCV encodes for a single polyprotein of approximately 3000 amino acids that is processed by the viral HCV protease enzyme into three structural proteins (HCV core, E1 and E2), six nonstructural proteins (NS2, NS3, NS4A, NS4B, NS5A, NS5B), and the p7 ion channel.[5] The nonstructural proteins are a combination of enzymes and cofactors that are responsible for proper viral replication. Much of the direct-acting antiviral drug development to date has focussed on the functionally well-characterised HCV protease (NS3) and polymerase (NS5B) enzymes, for which crystal structures are available.[6] The nonstructural protein 5A (NS5A) exists as basally and hyperphosphorylated forms that participate in viral replication via a replication complex and indeed has been shown to interact with a wide variety of cellular proteins. However, NS5A has no known enzymatic function, confounding efforts to accurately determine its function in viral replication.[7,8]

Several companies have identified inhibitors of NS5A as promising direct acting antivirals.[9] The most advanced of these is daclatasvir (**1**; BMS790052), a highly potent NS5A inhibitor that was discovered and developed by Bristol–Myers–Squibb and is currently in phase 3 clinical trials (Figure 1).[10,11] The impressive efficacy of daclatasvir was confirmed in a single ascending dose study with a mean 3.3 $\log_{10}$ drop in viral load in HCV patients 24 h post administration of a 100 mg dose and a mean 1.95 $\log_{10}$ drop in viral load just 6 h after dosing. This was confirmed in a phase 2 trial that confirmed the efficacy of a once daily regimen of daclatasvir in combination with pegylated interferon and ribavirin.[12] Recently, daclatasvir has been proposed to block both the synthesis of new viral genomes

[a] *T. D. Tran, F. Wakenhut, L. Watson, M. Paradowski, Dr. J. Milbank, F. Adam, D. Hay, J.-Y. Chiva, C. Nichols, Dr. D. C. Blakemore, Dr. D. C. Pryde*
Worldwide Medicinal Chemistry, Pfizer Global Research & Development
Ramsgate Road, Sandwich, Kent CT13 9NJ (UK)
E-mail: david.pryde@pfizer.com

[b] *Dr. C. Pickford, S. Shaw, Dr. M. Westby, C. Smith-Burchnell*
Antivirals Virology, Pfizer Global Research & Development
Ramsgate Road, Sandwich, Kent CT13 9NJ (UK)

[c] *I. Gardner, S. Dayal, Dr. A. Pike, R. Webster*
Pharmacokinetics, Dynamics & Metabolism
Pfizer Global Research & Development
Ramsgate Road, Sandwich, Kent CT13 9NJ (UK)

[d] *Dr. R. A. Brimage, R. Halstead, Dr. R. Glen, Dr. C. P. Wilson*
Peakdale Molecular Ltd.
Sheffield Road, Chapel-en-le-Frith, High Peak, SK23 0PG (UK)

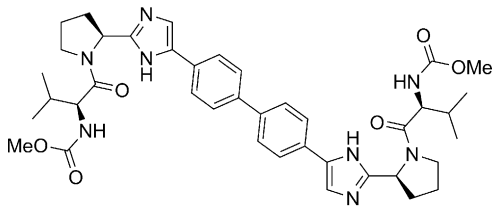

Daclatasvir (BMS790052) (**1**)
gt1b IC_{50}=10 pM; gt1a IC_{50}=47 pM

Figure 1. Daclatasvir (**1**), a clinically precedented HCV NS5A inhibitor.

and also to prevent the release of virus from infected cells, and it is this dual mode of action that is thought to be responsible for its high efficacy.[13] Given the exciting efficacy of NS5A inhibitors such as daclatasvir, we initiated our own programme aimed at finding a novel and highly potent agent, starting from daclatasvir itself. In our typical screening cascade, compound potency was assessed in subgenomic replicon cell lines within both a gt1b and gt1a background and for cytotoxicity in the same gt1b cell line.

At first glance, the most interesting aspects of **1** are its very high molecular size (MWt = 739) and dimeric topology. Molecular properties based on this type of structure would be predicted to be in higher risk chemical space for both absorption and solubility.[14] For our own programme, we were interested in evaluating the pharmacokinetic properties of analogues from this series as we progressed. Firstly, however, we embarked on scoping the structure–activity relationships (SARs) of the central biphenyl-imidazole unit of **1**, and in particular, monitored structural changes for their effects on both gt1b and gt1a potency in the replicon system.

For synthetic expedience, we initially based this study on the phenylglycine-pyrrolidine series shown in Table 1 in which simple modifications to the core structure resulted in sharp drops in cell-based potency, but also illustrated that these drops were not consistent for the two gt1 subtypes tested. For example, biphenyl parent structure **2** showed a balanced gt1 profile, albeit significantly weaker than **1**, while oxazole analogue **3** resulted in a significantly greater loss of activity against gt1a, but showed improved potency against gt1b. A number of linker groups were then inserted between the two phenyl rings, and again, resulted in a general loss of activity against the subtypes through incorporating a hydrocarbon (**4**), ether (**6**) or a contracted, fused naphthyl system (**7**). Interestingly, rigid unsaturated linking groups such as the alkynyl group in **5** did show a reduction in potency against both gt1 subtypes but did still retain a balanced activity profile. Our conclusion from this exercise was that the correct spatial arrangement of analogues of the biphenyl-imidazole system was key to achieving balanced gt1 activity, and that the initial data generated suggested this could be achievable in a novel linking structure, but that we had not identified an optimal linker as yet.

With this in mind, we then embarked upon a more focussed study of spacing groups that separated one of the imidazole rings from the remainder of the central linker in a number of different ways, as shown in Table 2. At this stage, we based all our subsequent designs on the prolyl-valinyl carbamate capping group, which we found to be uniformly more potent and in many cases offered improved permeability and oral bioavailability.[15] The 1,5-naphthyl analogue (**8**), an isomer of the 1,4-naphthyl system (**7**), was completely inactive against both gt1a and gt1b but, most intriguingly, the related 2,6-naphthyl analogue **13** was very potent, particularly against gt1b lending further weight to the importance of the molecular cores spatially presenting the remainder of the molecule correctly for balanced activity. Compound **13** was, however, both lipophilic and very poorly soluble, and we continued to seek analogues with better physicochemical properties. The level of potency of **13** was not reproduced in saturated ring-containing cores such as **9**, **10** and **12** or in alicyclic ether linkers such as **11**.

Saturated versions of the 2,6-naphthyl ring system were also investigated, for example, the tetrahydro-isoquinoline ring system in compound **14** that retained a reasonably balanced genotype profile but were significantly less active than the corresponding aromatic systems. The fully aromatic 2,6-naphthyl ring system (**13**) therefore became the most promising lead that was now pursued aggressively. Analogues of **13** are shown in Table 3.

Table 1. Structure and activities of phenylglycine-pyrrolidine analogues of the biphenyl-imidazole unit of **1**.[a]

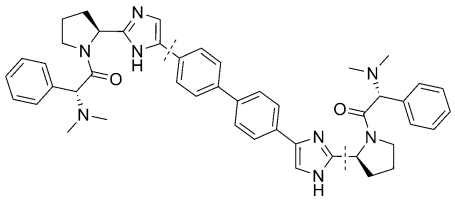

Compd	Structure	IC_{50} [pM][a] Replicon 1b	Replicon 1a	Cytotoxicity [nM][b]
2	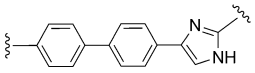	490	1190	> 500
3	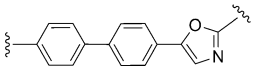	6	117000	6020
4	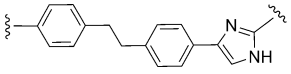	387	5700	> 500
5	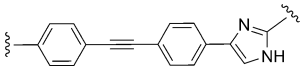	93	304	> 500
6	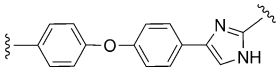	706	158000	> 500
7	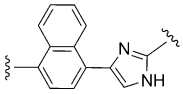	5020	500000	> 500

Data were determined in [a] a replicon cell-based assay or [b] a WST-1 cell proliferation assay and are the mean of at least two replicates.

Table 2. Structure and activities of analogues of the biphenyl-imidazole unit of **1**.[a]

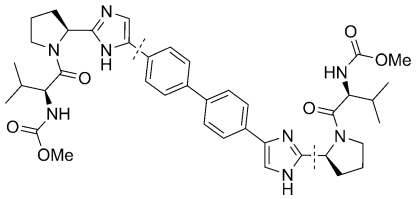

Compd	Structure	IC_{50} [pM][a] Replicon 1b	Replicon 1a	Cytotoxicity [nM][b]
1	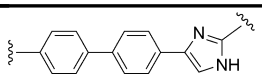	10	47	>500
8	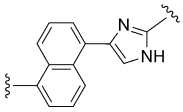	500 000	500 000	>500
9	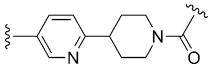	1200	257	>40 000
10	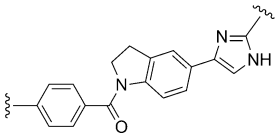	211	8840	>10
11	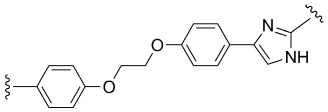	558	44 200	>24 800
12[c]	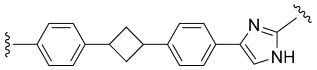	113	4470	>10
13	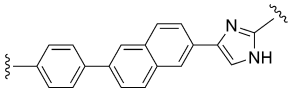	2	22	>40 000
14	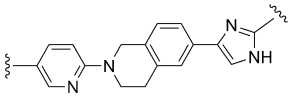	39	136	23 200

[a] Data were determined in [a] a replicon cell-based assay or [b] a WST-1 cell proliferation assay and are the mean of at least two replicates. [c] Compound **12** was prepared and evaluated as a mixture of *cis* and *trans* diastereoisomers at the cyclobutyl ring.

We were mindful of the high lipophilicity of compound **13** (cLog $P = 5.9$) and sought changes that lowered overall lipophilicity whilst retaining activity. Inserting nitrogen atoms into the naphthyl ring of **13** to decrease Log P gave compounds such as quinoline **16** (cLog $P = 4.8$) and quinazoline **15** (cLog $P = 3.9$) that both retained the excellent potency and subtype balance of **13**. Quinoxaline **17** (cLog $P = 4.1$) was particularly potent, with a gt1b IC_{50} value of 8 pM balanced with a similar gt1a IC_{50} value of 13 pM. Through adding the N atoms to this structure, the overall cLog P value of **17** was almost two units lower compared with starting naphthyl **13** and had an enhanced aqueous solubility (thermodynamic solubility of approximately 6 $\mu g\,mL^{-1}$, similar to that of **1**). Fused 6,5-bicyclic heterocycles displayed very subtle SAR as has been observed by others.[9a,15,16] While benzoxazole **18** and indazole **20** showed similar levels of potency and genotype balance to that of the starting naphthyl compound **13**, closely related benzothiazole **19** was at least two orders of magnitude less potent against gt1a. Separating the rings of a 6,5-bicycle as in phenyl oxadiazole **21** was not tolerated and was significantly weaker at both genotypes. Returning to very potent quinoxaline **17**, the rings of the 6,6-bicyclic system were separated and the phenyl ring fused to the adjacent imidazole. Similar strategies have recently been reported by others.[9a,15,17] Resulting pyrazine-benzimidazole **22** was of similar potency, albeit slightly weaker against genotype 1a, while the direct pyrimidine analogue **23** was slightly weaker again against genotype 1a. Pyridine analogues **24** and **25** were some fivefold less potent against genotype 1a than the phenyl equivalent. Moving the extra nitrogen atom onto the benzimidazole ring resulted in compounds that were less potent at both subtypes, with the 7-aza analogue (**27**) more balanced than the 4-aza analogue (**26**).

From the analogues prepared and profiled, a selection of the more potent and balanced agents were investigated alongside **1** for potency against several of the most common reported NS5A replicon-derived mutants[18] to emerge as shown in Table 4. In our systems, compound **1** displayed significant drops in activity, particularly within a gt1a background, with the M28T mutation showing a 350-fold drop in potency. Interestingly, the core-modified compounds described herein were all uniformly less sensitive to the gt1a mutations tested than **1** but against a gt1b background showed mixed results. While compound **17** showed a similar gt1b sensitivity as compound **1**, all other compounds tested were more sensitive to the L31V and the Y93H mutations. Whilst we have not generated any de novo resistance virus with any of the compounds described herein, our data are entirely consistent with the proposed mode of interaction of similar chemotypes across an NS5A dimer interface with the core structure proximal to the L31 amino acid location and the cap region to the Y93 amino acid location.[19]

These data were intriguing in that the peripheral substitution pattern of the analogues prepared in our study was identical to that of **1**, but significant differences in mutant sensitivity were seen.

We next turned our attention to evaluating the physicochemistry and pharmacokinetics of the series. When various properties of the compounds investigated were plotted in Figure 2, it appeared that microsomal metabolic stability across the Log D range was uniformly good in general. However, it also appeared that targeting a clog P value of around 4 or less would be beneficial for both permeability and for aqueous solubility. This focussed our attention on some of the less lipophilic analogues we had made, and we looked more closely at quinoxaline **17**.

Encouraged by the mutant profile and in vitro data of **17**, further in vitro and in vivo pharmacokinetic evaluation was undertaken as shown in Table 5. Compound **17** showed good passive permeability and low turnover in both human micro-

Table 3. Structure and activities of aromatic analogues of the 2,6-naphthyl lead (**13**).[a]

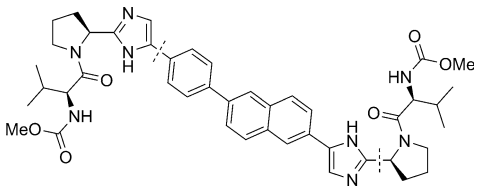

Compd	Structure	IC_{50} [пм][a] Replicon 1b	Replicon 1a	Cytotoxicity [нм][b]	Compd	Structure	IC_{50} [пм][a] Replicon 1b	Replicon 1a	Cytotoxicity [нм][b]
13	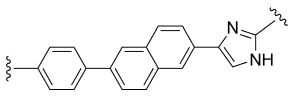	2	22	> 40 000	**21**	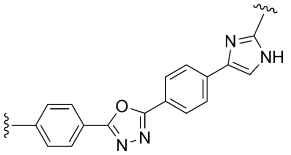	582	10 000	> 10
15	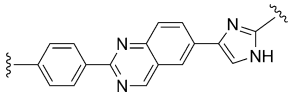	6	36	> 24 300	**22**	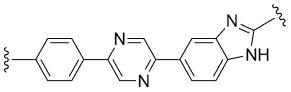	7	32	9800
16	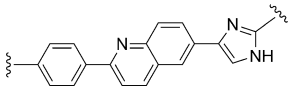	9	75	> 40 000	**23**	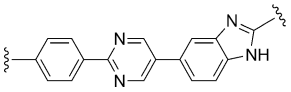	8	70	> 13 300
17	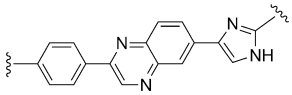	8	13	16 000	**24**	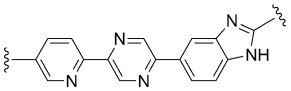	10	163	> 1000
18	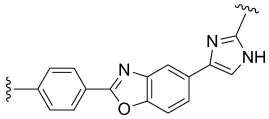	10	132	> 12 700	**25**	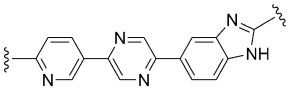	15	176	> 40 000
19	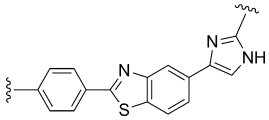	45	10 000	> 10	**26**	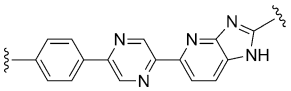	27	146	12 000
20	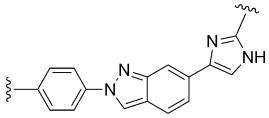	16	52	18 900	**27**	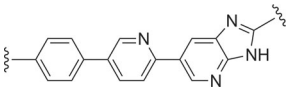	22	54	20 200

[a] Data were determined in [a] a replicon cell-based assay or [b] a WST-1 cell proliferation assay and are the mean of at least two replicates.

Table 4. Activity of selected compounds against mutant replicon cell lines, expressed as fold shift relative to wild type activity.

Compd	IC_{50} [пм] Replicon 1b	Replicon 1a	Shift (gt1b background) L31V	Y93H	Shift (gt1a background) M28T	Q30H
1	10	47	175	48.8	350	314
17	8	13	101	120	24.1	88.8
20	16	52	671	2180	38.8	263
22	7	32	1160	1410	33.1	66.6
23	8	70	3050	1110	9.95	62
24	10	163	393	1330	138	94.5
25	15	176	1270	3180	197	64.5
26	27	146	182	318	98.1	51.3
27	22	54	814	448	115	30.6

[a] Data were determined in a replicon cell based assay and are the mean of at least two replicates. Assay details are described in the Experimental Section.

somes and human hepatocytes. It was highly protein bound in all species and demonstrated significant efflux in a P-glycoprotein (Pgp)-overexpressing MDR-1 cell line. Metabolite studies indicated that any metabolite formation was overwhelmingly driven by CYP3A4 oxidative metabolism. In the rat, the compound showed low total clearance, was well absorbed, and had a short half-life.

The human pharmacokinetics of **17** were predicted to show low clearance ($CL < 0.3\ mL\ min^{-1}\ kg^{-1}$) and a long terminal half-life in excess of 24 h. These pharmacokinetic parameters were then used to translate into dose predictions based on a gt1a antiviral IC_{90} value for **17** of approximately 20 пм. It was predicted that a 10 mg dose would be sufficient to provide a free exposure at 24 h post-dosing of approximately 200 пм, some tenfold the antiviral IC_{90}, and **17** would therefore be suitable for once daily dosing. Compound **17** was evaluated in a rat exploratory toxicology study over 7 days at doses up to 500 $mg\ kg^{-1}$ with no adverse findings reported or histopathology abnormalities observed.

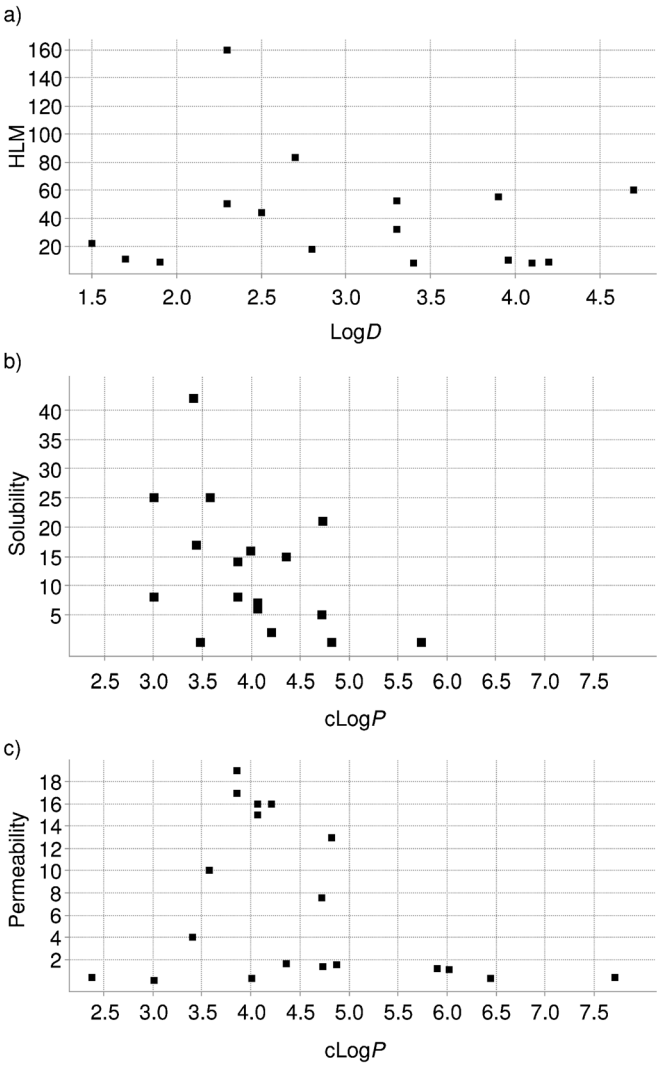

Figure 2. Physicochemical data correlate for compounds described in this paper, where data were measured: a) human liver microsomal (HLM) stability ($\mu L\,min^{-1}\,mg^{-1}$) versus measured log *D* in the top panel; b) aqueous solubility ($\mu g\,mL^{-1}$) plotted against calculated log *P* in the middle panel; c) passive permeability measured in a canine kidney cell line (10^{-6} cm s^{-1}) plotted against calculated log *P*. Solubility was measured from a DMSO stock solution using a kinetic miniaturized shake flask method.

In conclusion, through this study, we have identified novel core structures with a distinct resistance profile. Through a careful examination of in vitro physicochemical parameters, we have identified a compound that showed good absorption and a long predicted human pharmacokinetic half-life. Further investigations with compound **17** will be reported in due course.

Experimental Section

Discussion of synthesis

All compounds were synthesised in a similar manner. Representative syntheses of compounds **17** and **22** are shown in Schemes 1–5. For compound **17**, the molecule was synthesised from three key fragments as shown in Scheme 1.

Table 5. Selected in vitro parameters and in vivo rat pharmacokinetic parameters for compound **17**.

Parameter [unit]	Value
In vitro parameters[a]	
MW	791
*c*log *P* (log *D*)	4.1 (1.7)
hHeps [$\mu L\,min^{-1}\,million^{-1}$]	<2
RRCK[20] permeability AB/BA [10^{-6} cm s^{-1}]	16/13
HLM[21] [$\mu L\,min^{-1}\,mg^{-1}$]	<8
RLM [$\mu L\,min^{-1}\,mg^{-1}$]	<8
Human fu [%]	0.3
MDR-1[22] (AB/BA)	3.5/41
Rat pharmacokinetic parameters[b]	
CL [$mL\,min^{-1}\,kg^{-1}$]	14
CL_u [$mL\,min^{-1}\,kg^{-1}$]	3889
V_{dss} [$L\,kg^{-1}$]	2
$t_{1/2}$ [h]	2
F [%]	31

[a] All metabolism assays were conducted as described in Reference [21]. Permeability assays were conducted as described in References [20] and [22], as indicated. [b] Dose: 1 mg kg^{-1} (i.v.); 2 mg kg^{-1} (p.o.); cremaphor vehicle.

The syntheses of the three fragments are shown in Scheme 2. Bromoimidazole **28** was synthesised starting from Boc-L-proline **31**. The proline was converted to aldehyde **33** via reduction to the alcohol **32** followed by TEMPO/bleach oxidation. The aldehyde was sensitive to epimerisation but this sequence proved most effective for maintaining chiral integrity. The aldehyde was converted to imidazole **34** using ammonia and glyoxal, and the imidazole NH was protected with a [2-(trimethylsilyl)ethoxy]methyl (SEM) group to give imidazole **35**. Bromination occurred selectively at the 5-position of the imidazole, with the presence of the electron-withdrawing SEM group preventing over bromination to give **28**. Imidazole boronate **29** was synthesised starting from Boc-L-proline **31** and bromoketone **36**. The resulting ketoester (**37**) was rearranged to imidazole **38** using ammonium acetate in xylene; this was converted to boronate ester **29** under palladium-mediated conditions with bis(pinacolato)diboron. Finally, quinoxaline fragment **30** was synthesised starting from quinoxalinone **39**. Selective bromination at the 6-position of the quinoxaline could be accomplished under silver-mediated conditions to give **40**; this was then treated with $POCl_3$ giving the desired quinoxaline fragment (**30**).

To put the three key fragments together, the approach shown in Scheme 3 was followed. Quinoxaline **30** was Suzuki coupled with imidazole boronate **29** to give bromoquinoxaline **41**. Key to the success of our strategy was the selective coupling at the 2-chloro position rather than the 6-bromo position, and we found that Pd(dppf)Cl_2 at room temperature effected this transformation with excellent regioselectivity. Subsequent boronate ester formation was followed by a second Suzuki coupling with bromoimidazole **28** to give **43**. To access compound **17**, all that remained was to deprotect the SEM and Boc groups and carry out a double amide bond formation using 1-ethyl-3-(3-dimethylaminopropyl)carbodiimide (EDCI), hydroxybenzotriazole (HOBt) and protected valine **45**. This sequence gave **17** without loss of chiral integrity.[23]

For compound **22**, a similar strategy was utilised with the molecule being built from three key fragments (Scheme 4). Imidazoleboro-

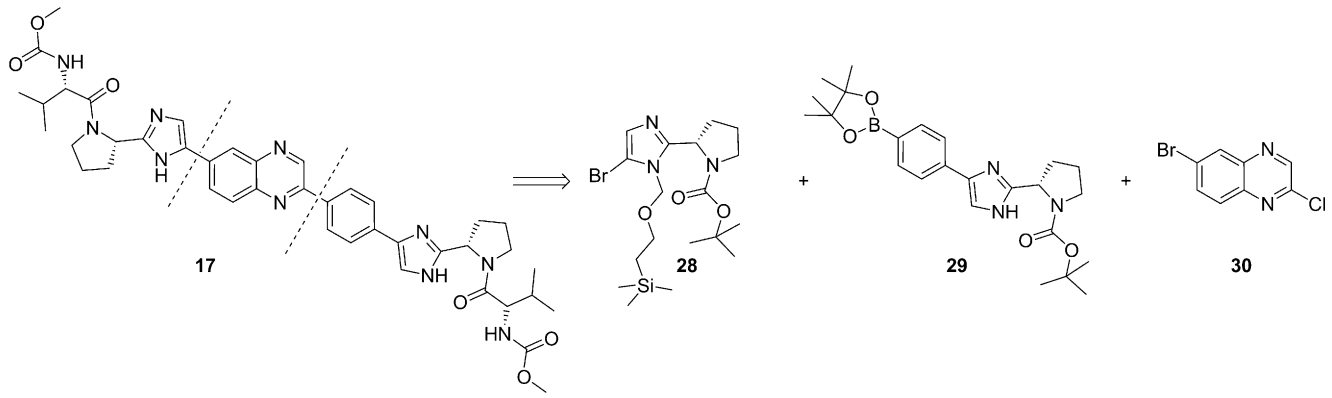

Scheme 1. Synthetic strategy towards compound **17**.

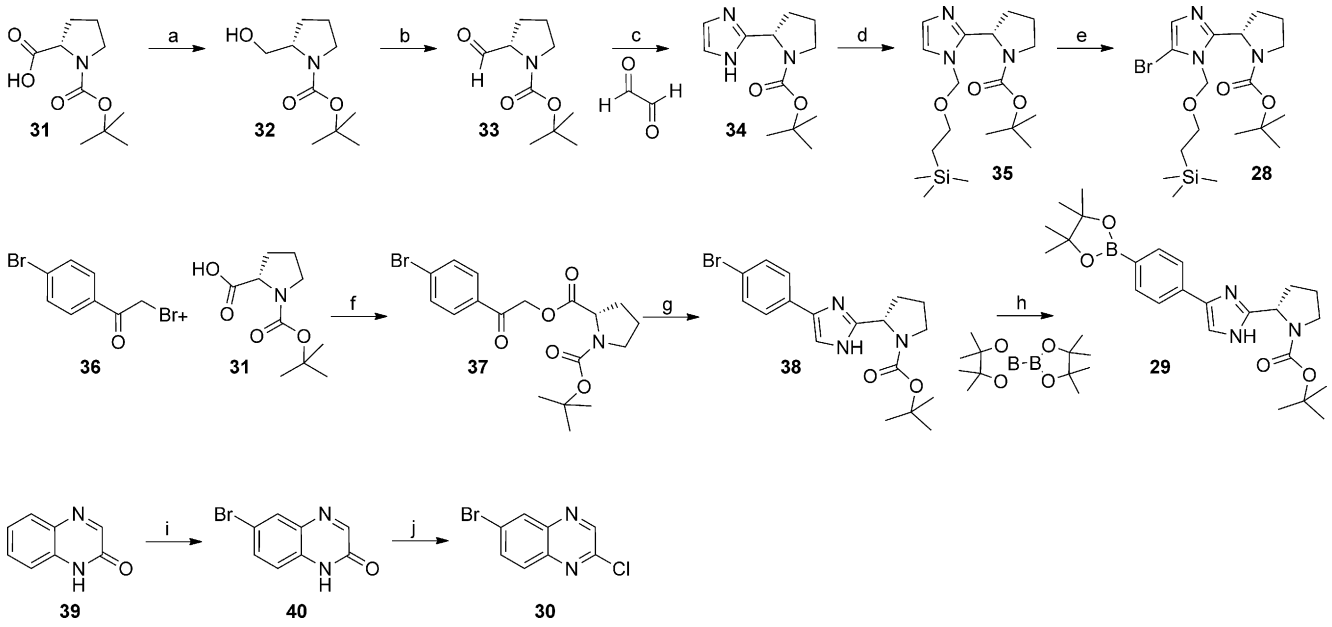

Scheme 2. Synthesis of key fragments for making **17**. *Reagents and conditions*: a) BH_3·THF, THF, 0 °C→RT, 100%; b) TEMPO, NaOCl, NaBr, $NaHCO_3$, CH_2Cl_2/H_2O, 0 °C, 86%; c) NH_3(aq), MeOH, RT, 65%; d) NaH, *N*-methylpyrrolidine, 0 °C then SEMCl, 80%; e) NBS, CH_2Cl_2, RT, 99%; f) DIPEA, CH_2Cl_2, RT, 100%; g) NH_4OAc, xylene, 150 °C, 79%; h) Pd(dppf)Cl_2·CH_2Cl_2, KOAc, dioxane, 100 °C, 73%; i) Br_2, Ag_2SO_4, H_2SO_4, $CHCl_3$, 90%; j) $POCl_3$, DMF, 90%.

nate **29** was synthesised as for the previous compound. Benzimidazole boronate **46** was synthesised from Boc-L-proline **31** as shown in Scheme 5. Amide coupling to generate **48** was followed by ring closure under acidic conditions to give bromobenzimidazole **49**. This was converted to boronate ester **46** under palladium-mediated conditions with bis(pinacolato)diboron.

To complete the synthesis, all that was needed was the selective coupling of boronates **29** and **46** with the pyrazine (Scheme 6). Benzimidazole boronate **46** was coupled with 2-bromo-5-iodopyrazine **47** under palladium-mediated conditions to give **50** in good yield; use of the 2-bromo-5-iodopyrazine proved optimal for minimising double addition in this reaction. Bromopyrazine **50** was then Suzuki coupled with boronate **29** and, following deprotection and double amide coupling, the desired product **22** was obtained.[24] Again, no loss of chiral integrity was seen in this sequence.

Screening methods

Determination of HCV 1a replicon inhibitory activity: Genotype 1a (H77, licensed from Apath LLC) HCV replicon cells were resuspended to a concentration of 1.4×10^5 cells mL^{-1} by addition of prewarmed assay medium (DMEM + 10% FCS). A 45 μL aliquot of this suspension was added to each well of a 384-well assay plate (Lumitrac, Greiner) already containing 0.5 μL of test compound. All plates were covered with gas-permeable seals and incubated at 37 °C, 5% CO_2 for 48 h. After 48 h, the assay plate was removed from the incubator and left to cool to RT for 15–30 min. Medium was removed from the wells, and 5 μL lysis buffer (Renilla Luciferase Assay Kit, Promega) was added to each well. The plate was incubated at RT on a rocker for 15 min, then 15 μL Assay Substrate was added to each well. Luminescence was read immediately using an EnVision plate reader.

Determination of HCV 1b replicon inhibitory activity: Genotype 1b (con1, licensed from Reblikon GmbH) HCV replicon cells were resuspended to a concentration of 1.4×10^5 cells mL^{-1} by addition of

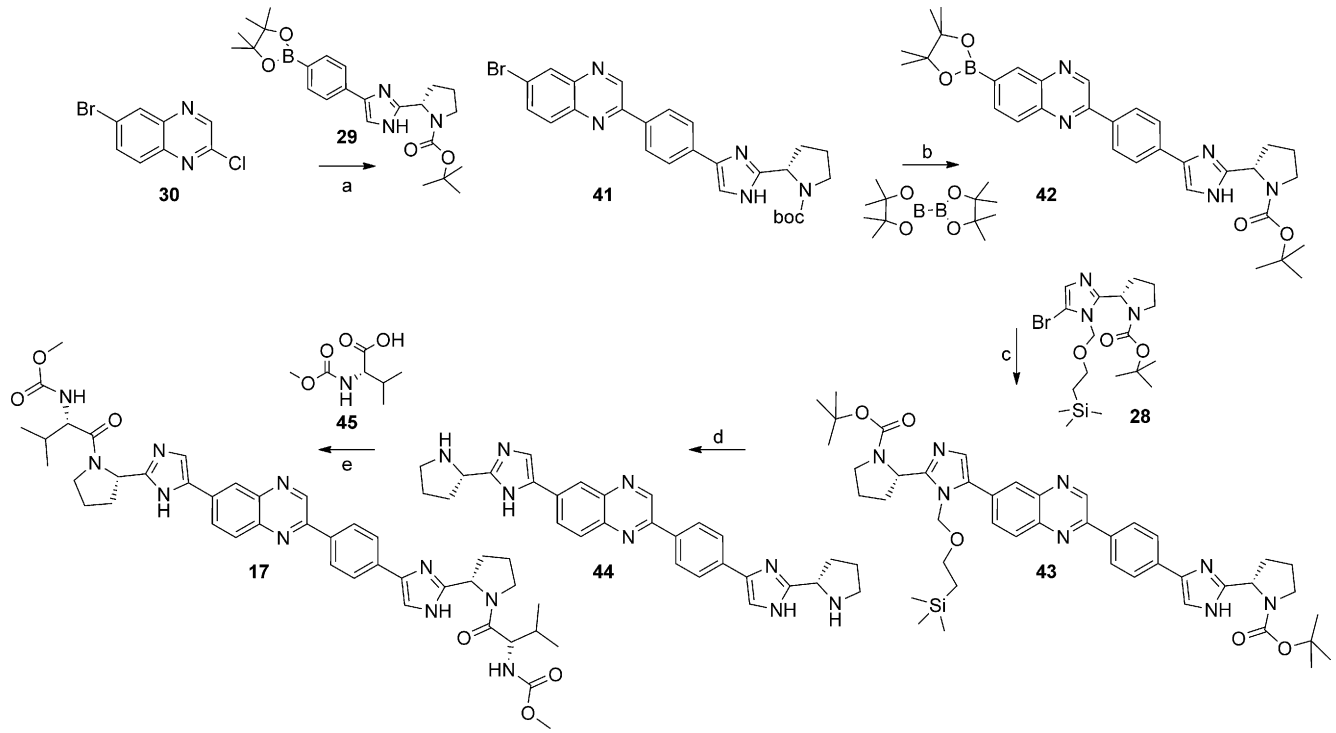

Scheme 3. End-game for the synthesis of **17**. *Reagents and conditions*: a) $Pd(dppf)Cl_2$, Na_2CO_3, DME, RT, 76%; b) $Pd(dppf)Cl_2$, KOAc, 1,4-dioxane, reflux, 71%; c) $Pd(dppf)Cl_2$, Na_2CO_3, DME, reflux, 60%; d) 4 N HCl, dioxane, EtOH, 75 °C, 92%; e) EDCI, HOBt, DIPEA, CH_3CN, RT, 71%.

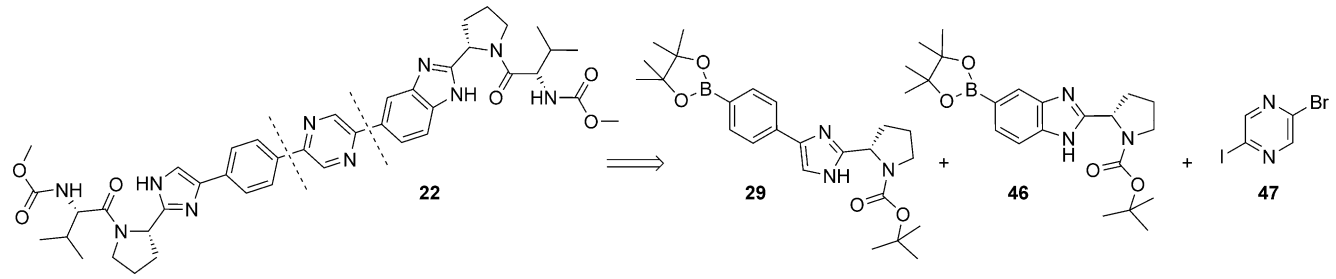

Scheme 4. Synthetic strategy towards **22**.

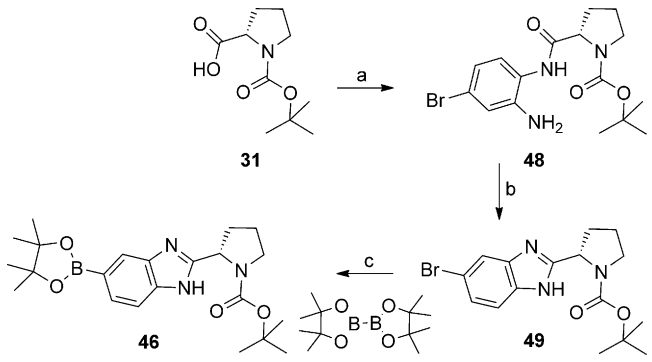

Scheme 5. Synthesis of benzimidazole boronate **46**. *Reagents and conditions*: a) 2-Amino-4-bromo-aniline, HBTU, DIPEA, CH_2Cl_2, RT, 100%; b) AcOH, 70 °C, 75%; c) $Pd(dppf)Cl_2$, KOAc, dioxane, reflux, 79%.

pre-warmed medium (DMEM + 10% FCS). A 45 μL aliquot of this suspension was added to each well of a 384-well assay plate (Lumitrac, Greiner) already containing 0.5 μL of test compound. All plates were covered with gas-permeable seals and incubated at 37 °C, 5% CO_2 for 48 h. After 48 h, the plate was removed from the incubator and left to cool to RT for 15–30 min. An equal volume of reconstituted Lyophilised Britelite Plus Substrate (PerkinElmer) to medium was added to each well. Luminescence was read immediately on an EnVision (PerkinElmer) plate reader.

Determination of inhibitor induced cytotoxicity in HCV replicon cell lines: Genotype 1b (con1) HCV replicon cells were resuspended to a concentration of 1.4×10^5 cells mL^{-1} by addition of pre-warmed medium (DMEM + 10% FCS). A 45 μL aliquot of this suspension was added to each well of a 384-well assay plate (Greiner) already containing 0.5 μL of test compound. All plates were covered with gas-permeable seals and incubated at 37 °C, 5% CO_2 for 48 h. After 48 h, 5 μL of WST-1 cell proliferation reagent (Roche) was added to each well, and the plate returned to the incubator for 1 h. After this incubation period, absorbance was read at 450 nm on an EnVision (PerkinElmer) plate reader.

Determination of resistant HCV replicon inhibitory activity: Resistance mutations were introduced to genotype 1b (con1, licenced from Apath LLC) and 1a (H77, Apath LLC) replicons using the Quik-

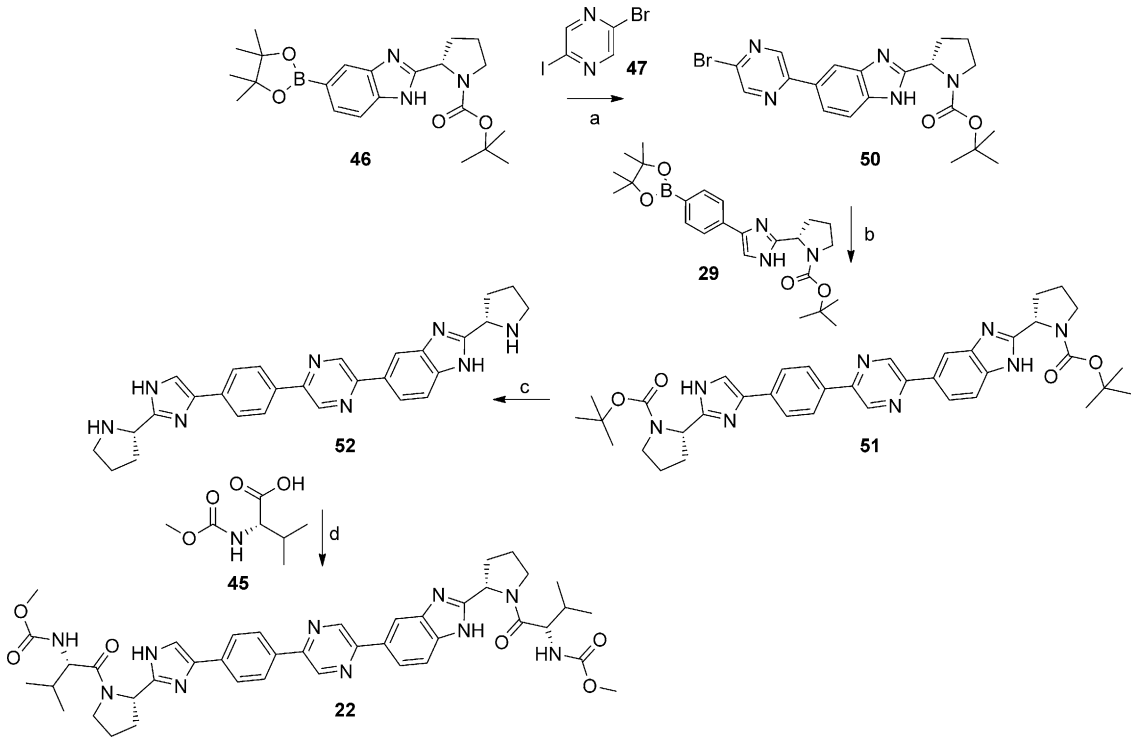

Scheme 6. End-game for the synthesis of **22**. *Reagents and conditions*: a) $Pd(dppf)Cl_2$, Na_2CO_3, toluene/EtOH/H_2O, 60 °C, 72%; b) $Pd_2(dba)_3$, PCy_3, K_3PO_4, dioxane, 100 °C, 55%; c) HCl, EtOH, 90 °C, 87%; d) HOBt, EDCI, CH_3CN, DIPEA, 0 °C→RT, 42%.

change XL (Stratagene). NS5A L31V and Y93H were introduced to genotype 1b, and the M28T and Q30H mutations were introduced to genotype 1a replicons. Wild-type or mutant replicons were transiently transfected into Huh-7.5 cells (Licensed from Apath LLC) using an Amaxa Nucleofector (Lonza group Ltd). Following transfection, the cells were resuspended to a concentration of 5.3×10^4 cells mL^{-1} per in assay medium (DMEM + 10% FCS). A 180 μL aliquot of cell suspension was added to each well of a 96-well white assay plate (Costar, Corning Inc.), and plates were incubated overnight at 37 °C, 5% CO_2. Following this incubation, 20 μL of compound diluted in assay medium were added. All plates were covered with gas-permeable seals and incubated at 37 °C, 5% CO_2 for 72 h. After 72 h, the assay plate was removed from the incubator and left to cool to RT for 15–30 min. Medium was removed from the wells, and 5 μL lysis buffer (Renilla Luciferase Assay Kit, Promega) was added to each well. The plate was incubated at RT on a rocker for 15 min, then 15 μL Assay Substrate was added to each well. Luminescence was read immediately using an EnVision plate reader.

Acknowledgements

The authors thank Dr. Gavin Whitlock for helpful discussions throughout the course of this work, and Ms. Jenny Middleton and Mr. Malcolm Macartney for help with virology assessments.

Keywords: antiviral agents · drug resistance · HCV · hepatitis C virus · NS5A · viral proteases

[1] D. Lavanchy, *Liver Int.* **2009**, *29*, 74–81.
[2] R. S. Brown, *Nature* **2005**, *436*, 973–978.
[3] J. H. Hoofnagle, L. B. Seeff, *N. Engl. J. Med.* **2006**, *355*, 2444–2451.
[4] T. J. Liang, M. G. Ghany, *N. Engl. J. Med.* **2013**, *368*, 1907–1917.
[5] T. P. Holler, T. Parkinson, D. C. Pryde, *Expert Opin. Drug Discovery* **2009**, *4*, 293–314.
[6] J. J. Kiser, C. Flexner, *Annu. Rev. Pharmacol. Toxicol.* **2013**, *53*, 427–449.
[7] O. Belda, P. Targett-Adams, *Virus Res.* **2012**, *170*, 1–14.
[8] M. Belema, O. D. Lopez, J. A. Bender, J. L. Romine, D. R. St. Laurent, D. R. Langley, J. A. Lemm, D. R. O'Boyle, J-H. Sun, C. Wang, R. A. Fridell, N. A. Meanwell, *J. Med. Chem*, **2014**, *57*, 1643–1672.
[9] For recent disclosures of NS5A inhibitors, see a) C. A. Coburn, P. T. Meinke, W. Chang, C. M. Fandozzi, D. J. Graham, B. Hu, Q. Huang, S. Kargman, J. Kozlowski, R. Liu, J. A. McCauley, A. A. Nomeir, R. M. Soll, J. P. Vacca, D. Wang, H. Wu, B. Zhong, D. B. Olsen, S. W. Ludmerer, *ChemMedChem* **2013**, *8*, 1930–1940; b) M. Belema, V. N. Nguyen, D. R. St. Laurent, O. D. Lopez, Y, Qiu, A. C. Good, P. T. Nower, L. Valera, D. R. O'Boyle, J.-H. Sun, M. Liu, R. A. Fridell, J. A. Lemm, M. Gao, J. O. Knipe, N. A. Meanwell, L. B. Snyder, *Bioorg. Med. Chem. Lett.* **2013**, *23*, 4428–4435.
[10] J. A. Lemm, J. E. Leet, D. R. O'Boyle, J. L. Romine, X. S. Huang, D. R. Schroeder, J. Alberts, J. L. Cantone, J.-H. Sun, P. T. Nower, S. W. Martin, M. H. Serrano-Wu, N. A. Meanwell, L. B. Snyder, M. Gao, *Antimicrob. Agents Chemother.* **2011**, *55*, 3795–3802.
[11] M. Gao, R. E. Nettles, M. Belema, L. B. Snyder, V. N. Nguyen, R. A. Fridell, M. H. Serrano-Wu, D. R. Langley, J.-H. Sun, D. R. O'Boyle, J. A. Lemm, C. Wang, J. O. Knipe, C. Chien, R. J. Colonno, D. M. Grasela, N. A. Meanwell, L. G. Hamann, *Nature* **2010**, *465*, 96–100.
[12] S. Pol, R. H. Ghalib, V. K. Rustgi, C. Martorell, G. T. Everson, H. A. Tatum, C. Hezode, J. K. Lim, J.-P. Bronowicki, G. A. Abrams, N. Brau, D. W. Morris, P. J. Thuluvath, R. W. Reindollar, P. D. Yin, U. Diva, R. Hindes, F. McPhee, D. Hernandez, M. Wind-Rotolo, E. A. Hughes, S. Schnittman, *Lancet Infect. Dis.* **2012**, *12*, 671–677.
[13] J. Guedj, H. Dahari, L. Rong, N. D. Sansone, R. E. Nettles, S. J. Cotler, T. J. Layden, S. L. Uprichard, A. S. Perelson, *Proc. Natl. Acad. Sci. USA* **2013**, *110*, 3991–3996.
[14] P. D. Leeson, B. Springthorpe, *Nat. Rev. Drug Discovery* **2007**, *6*, 881–890.
[15] M. Belema, V. N. Nguyen, C. Bachand, D. H. Deon, J. T. Goodrich, C. A. James, R. Lavoie, O. D. Lopez, A. Martel, J. L. Romine, E. H. Ruediger,

L. B. Snyder, D. R. St. Laurent, F. Yang, J. Zhu, H. S. Wong, D. R. Langley, S. P. Adams, G. H. Cantor, A. Chimalakonda, A. Fura, B. M. Johnson, J. O. Knipe, D. D. Parker, K. S. Santone, R. A. Fridell, J. A. Lemm, D. R. O'Boyle, R. Colonno, M. Gao, N. A. Meanwell, L. G. Hamann, *J. Med. Chem*, **2014**, 57, 2013 – 2032.

[16] D. A. DeGoey, J. T. Randolph, D. Liu, J. Pratt, C. Hutchins, P. Donner, A. C. Krueger, M. Matulenko, S. Patel, C. E. Motter, L. Nelson, R. Keddy, M. Tufano, D. D. Caspi, P. Krishnan, N. Mistry, G. Koev, T. J. Reisch, R. Mondal, T. Pilot-Matias, Y. Gao, D. W. A. Beno, C. J. Maring, A. Molla, E. Dumas, A. Campbell, L. Williams, C. Collins, R. Wagner, W. M. Kati, *J. Med. Chem*, **2014**, 57, 2047 – 2057.

[17] J. O. Link, J. G. Taylor, L. Xu, M. Mitchell, H. Guo, H. Liu, D. Kato, T. Kirschberg, J. Sun, N. Squires, J. Parrish, T. Keller, Z-Y. Yang, C. Yang, M. Matles, Y. Wang, K. Wang, G. Cheng, Y. Tian, E. Mogolian, E. Mondou, M. Cornpropst, J. Perry, M. C. Desai, *J. Med. Chem*. **2014**, 57, 2033 – 2046.

[18] R. A. Fridell, D. Qiu, C. Wang, L. Valera, M. Gao, *Antimicrob. Agents Chemother.* **2010**, *54*, 3641 – 3650.

[19] D. R. O'Boyle II, J.-H. Sun, P. T. Nower, J. A. Lemm, R. A. Fridell, C. Wang, J. L. Romine, M. Belema, V. N. Nguyen, D. R. St. Laurent, M. Serrano-Wu, L. B. Snyder, N. A. Meanwell, D. R. Langley, M. Gao, *Virology* **2013**, *444*, 343 – 354.

[20] L. Di, C. Whitney-Pickett, J. P. Umland, H. Zhang, X, Zhang, D. E. Gebhard, Y. Lai, J. J. Federico, R. E. Davidson, R. Smith, E. L. Reyner, C. Lee, B. Feng, C. Rotter, M. V. Varma, S. Kempshall, K. Fenner, A. F. El-Kattan, T. E. Liston, M. D. Troutman, *J. Pharm. Sci.* **2011**, *100*, 4974 – 4985.

[21] G. Allan, J. Davis, M. Dickins, I. Gardner, T. Jenkins, H. Jones, R. Webster, H. Westgate, *Xenobiotica* **2008**, *38*, 620 – 640.

[22] B. Feng, J. B. Mills, R. E. Davidson, R. J. Mireles, J. S. Janiszewski, M. D. Troutman, S. M. de Morais, *Drug Metab. Dispos.* **2008**, *36*, 268 – 275.

[23] Methyl ((*S*)-1-((*S*)-2-(4-(4-(6-(2-((*S*)-1-((methoxycarbonyl)-L-valyl)pyrrolidin-2-yl)-1*H*-imidazol-5-yl)quinoxalin-2-yl)phenyl)-1*H*-imidazol-2-yl)pyrrolidin-1-yl)-3-methyl-1-oxobutan-2-yl)carbamate (**17**): ^{1}H NMR (400 MHz, CD_3OD): δ = 9.35–9.20 (m, 1H), 8.40–7.60 (m, 7H), 7.55–7.30 (m, 2H), 5.40–5.15 (m, 2H), 4.30–4.20 (m, 2H), 4.15–3.85 (m, 4H), 3.68–3.62 (m, 6H), 2.50–1.90 (m, 10H), 1.00–0.80 ppm (m, 12H); MS (ESI): m/z = 791 $[M+H]^+$.

[24] Methyl ((*S*)-1-((*S*)-2-(5-(5-(4-(2-((*S*)-1-((methoxycarbonyl)-L-valyl)pyrrolidin-2-yl)-1*H*-imidazol-4-yl)phenyl)pyrazin-2-yl)-1*H*-benzo[*d*]imidazol-2-yl)-pyrrolidin-1-yl)-3-methyl-1-oxobutan-2-yl)carbamate (**22**): ^{1}H NMR (400 MHz, CD_3OD): δ = 8.30–7.25 (m, 9H), 7.10–7.00 (m, 1H), 5.35–5.10 (m, 2H), 4.35–4.20 (m, 2H), 4.15–3.85 (m, 4H), 3.68–3.62 (m, 6H), 2.50–1.90 (m, 10H), 1.00–0.80 ppm (m, 12H); MS (ESI): m/z = 791 $[M+H]^+$.

Received: January 20, 2014
Published online on ■■ ■■, 0000

COMMUNICATIONS

*T. D. Tran, F. Wakenhut, C. Pickford, S. Shaw, M. Westby, C. Smith-Burchnell, L. Watson, M. Paradowski, J. Milbank, R. A. Brimage, R. Halstead, R. Glen, C. P. Wilson, F. Adam, D. Hay, J.-Y. Chiva, C. Nichols, D. C. Blakemore, I. Gardner, S. Dayal, A. Pike, R. Webster, D. C. Pryde**

■■ – ■■

The Discovery of Potent Nonstructural Protein 5A (NS5A) Inhibitors with a Unique Resistance Profile—Part 1

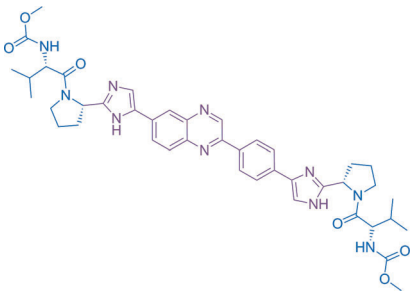

Resisting resistance: An investigation into the anti-hepatitis C virus (HCV) replicon activity of a series of biaryl-linked pyrrolidine NS5A inhibitors explored a diverse range of core structure modifications as key determinants of antiviral activity and susceptibility to common resistance mutations. Further evaluation of several core structure designs identified a compound with excellent pharmacokinetics, suitable for once daily dosing.